NRC·CNRC

NRC Publications Archive
Archives des publications du CNRC

Temperature dependence and gas-sensing response of conduction for mixed conducting SrFeyCozOx thin films

Tunney, Jim; Post, Michael; Du, Xiaomei; Yang, Dongfang

This publication could be one of several versions: author's original, accepted manuscript or the publisher's version. / La version de cette publication peut être l'une des suivantes : la version prépublication de l'auteur, la version acceptée du manuscrit ou la version de l'éditeur.
For the publisher's version, please access the DOI link below./ Pour consulter la version de l'éditeur, utilisez le lien DOI ci-dessous.

Publisher's version / Version de l'éditeur:
https://doi.org/10.1149/1.1470661
Journal of the Electrochemical Society, 149, 6, pp. H113-H118, 2002

NRC Publications Record / Notice d'Archives des publications de CNRC:
https://nrc-publications.canada.ca/eng/view/object/?id=8ab5c16d-e836-4ab3-9716-c180e5058d94
https://publications-cnrc.canada.ca/fra/voir/objet/?id=8ab5c16d-e836-4ab3-9716-c180e5058d94

Access and use of this website and the material on it are subject to the Terms and Conditions set forth at
https://nrc-publications.canada.ca/eng/copyright
READ THESE TERMS AND CONDITIONS CAREFULLY BEFORE USING THIS WEBSITE.

L'accès à ce site Web et l'utilisation de son contenu sont assujettis aux conditions présentées dans le site
https://publications-cnrc.canada.ca/fra/droits
LISEZ CES CONDITIONS ATTENTIVEMENT AVANT D'UTILISER CE SITE WEB.

Questions? Contact the NRC Publications Archive team at PublicationsArchive-ArchivesPublications@nrc-cnrc.gc.ca. If you wish to email the authors directly, please see the first page of the publication for their contact information.

Vous avez des questions? Nous pouvons vous aider. Pour communiquer directement avec un auteur, consultez la première page de la revue dans laquelle son article a été publié afin de trouver ses coordonnées. Si vous n'arrivez pas à les repérer, communiquez avec nous à PublicationsArchive-ArchivesPublications@nrc-cnrc.gc.ca.

National Research Council Canada | Conseil national de recherches Canada

Canada

Journal of The Electrochemical Society, **149** (6) H113-H118 (2002)
0013-4651/2002/149(6)/H113/6/$7.00 © The Electrochemical Society, Inc.

Temperature Dependence and Gas-Sensing Response of Conduction for Mixed Conducting $SrFe_yCo_zO_x$ Thin Films

James J. Tunney,*,z Michael L. Post,* Xiaomei Du, and Dongfang Yang

Institute for Chemical Process and Environmental Technology, National Research Council of Canada, Ottawa, Ontario K1A 0R6, Canada

A series of $SrFe_yCo_zO_x$ thin films on sapphire substrates was prepared by laser deposition and the conductance responses to both temperature and gas composition in O_2/N_2 mixtures were examined. All films exhibited p-type semiconductor behavior with film conductivities at 500°C between 20 and 200 S/cm for films exposed to 100% O_2 atm and 0.4-25 S/cm for films exposed to 0.2% O_2. At 500°C, thin films of compositions $SrFe_yCo_{1-y}O_x$, $0.25 \leqslant y \leqslant 0.75$, were found to be the most conductive for oxygen partial pressures between $0.002 < p_{O_2} < 1.0$ atm. $SrFeO_x$ and $SrFe_{1.3}Co_{0.2}O_x$ films were found to be the least conductive under these conditions. $SrFe_{0.25}Co_{0.75}O_x$ and $SrFe_{0.5}Co_{0.5}O_x$ films were found to exhibit regions where conductivity exhibited temperature independence between $200 \leqslant T \leqslant 500$°C for oxygen concentrations between 0.2 and 100% O_2. The temperature independence was interpreted as the result of a balancing of two opposing thermal effects: thermal activation of charge carriers and thermal-induced oxygen stoichiometry changes. For some films, enhanced oxygen sensitivity was observed over narrow p_{O_2} regions, and is attributed to cubic perovskite to brownmillerite phase transitions. CO and H_2 gases could be detected in background air for conditions where there is negligible temperature dependence of conduction.
© 2002 The Electrochemical Society. [DOI: 10.1149/1.1470661] All rights reserved.

Manuscript submitted April 23, 2001; revised manuscript received December 17, 2001. This was Paper 894 presented at the Phoenix, Arizona, Meeting of the Society, October 22-27, 2000. Available electronically April 12, 2002.

Mixed conducting ceramic materials of the type $SrFe_yCo_zO_x$ are characterized by their oxygen nonstoichiometry and their high electronic and ionic conductivities.[1-15] Consequently, they are suitable candidate materials for applications such as oxygen separation membranes, electrode materials for solid oxide fuel cells, and solid-state chemical sensors. It has been reported that some $SrFe_yCo_{1-y}O_x$ materials have oxygen ion mobilities greater than yttria-stabilized zirconia (YSZ) below 800°C.[1-3,7] Recently, the high oxygen ion mobility of the $SrFe_yCo_{1.5-y}O_x$ ($1.0 < y < 1.5$) composition[8-17] has been attributed to the perovskite-type $SrFe_yCo_{1-y}O_x$ phase.[8]

It has previously been shown that perovskite-based ceramic materials which exhibit p-type semiconductivity and mixed conductivity may be suitable candidates for temperature-independent gas sensors.[18-21] The basis for this temperature independence is the balancing of two separate thermal effects. The first effect is related to the thermal activation of charge carriers and is described in Eq. 1[18]

$$\sigma = \sigma_0 \exp(-E_A/kT) \quad [1]$$

An Arrhenius relationship exists between the conductivity of the material (σ) and the temperature (T) and is characterized by an activation energy E_A. For a p-type semiconductor, an increase in temperature normally results in increased conductivity caused by an increase in the number of hole electronic carriers in the conduction band. This results from the thermal excitation of electrons from the conduction band to a higher energy band. The second thermal effect is related to the oxygen nonstoichiometric properties of some perovskite materials. A temperature increase for a constant O_2 partial pressure in the gas phase over the solid results in some degree of oxygen evolution and an associated reduction of the material

$$O^x \rightarrow V_o^{\bullet\bullet} + 2e^- + \frac{1}{2}O_2\uparrow \quad [2]$$

Equation 2 describes the removal of an oxygen atom from an oxygen site, O^x, yielding two electrons, a doubly charged oxygen vacancy, $V_o^{\bullet\bullet}$, and O_2 gas. The electrons which are produced by the evolution of oxygen combine with the dominant electronic hole carriers, decreasing the conductivity of the material.

Under certain circumstances it has been shown that it is possible to balance these two opposing thermal effects so that the resistance response of the semiconductor material is effectively temperature independent. This has been examined with the goal of developing temperature-independent gas sensors.[18-21] Williams *et al.* examined a series of ferrates including $BaFe_{1-x}Ta_xO_3$, which showed negligible conductivity dependence to temperature, between 600 and 800°C.[18-20] More recently, Moos *et al.* demonstrated that acceptor- and donor-doped $SrTi_{1-x}Fe_xO_{3-\delta}$ materials could be tailored to yield temperature-independent conductivity responses between 700 and 900°C.[21] These materials were being investigated for applications as oxygen sensors for combustion exhaust control.

Thick-film perovskite materials were used for all these studies, and the temperature-independent regions were above 500°C. Thin films provide advantages related to the higher surface area-to-volume ratio. Thinner films of gas sensors based on a bulk equilibration mechanism between the film and the gas mixture provide faster response times. Previous work has shown that it is possible to grow high-quality thin films of $SrFeO_x$ ($2.5 \leqslant x \leqslant 3.0$) using pulsed laser deposition (PLD), which shows oxygen-sensing properties between $350 < T < 500$°C.[22-25]

For some gas-sensing applications, it would be advantageous to use transducer materials which exhibit a temperature-independent resistance response at lower temperatures and still demonstrate adequate gas sensitivity. In this study, $SrFe_yCo_zO_x$ materials grown as thin films are shown to have reversible bulk oxygen equilibration properties which may be exploited to achieve a conductivity response for O_2, CO, and H_2 sensing, which has a negligible temperature dependence.

Experimental

All $SrFe_yCo_zO_x$ materials were prepared as sintered pellets using standard ceramic techniques.[22-25] High-purity (>99.99%) $SrCO_3$, Fe_2O_3, and Co_3O_4 materials were mixed in the required ratios, followed by thermal treatments in flowing argon and/or oxygen at 1050-1100°C. These materials were then pressed into 12 mm diam targets followed by sintering at 1000-1150°C under flowing oxygen. The pellets were all verified to be single phase by X-ray diffraction (XRD) before being used as targets for pulsed laser ablation deposition (PLD). The X-ray spectra were indexed according to previously determined crystal structures. $SrFe_yCo_{1-y}O_x$ ($y = 0.25$, 0.5, 0.75, 0.9, 1.0) were indexed to the cubic perovskite structure,[26-28] $SrCoO_x$ to the hexagonal structure,[29] and $SrFe_{1.0}Co_{0.5}O_x$ and

* Electrochemical Society Active Member.
z E-mail: jim.tunney@nrc.ca

Downloaded 03 Jun 2009 to 132.246.79.102. Redistribution subject to ECS license or copyright; see http://www.ecsdl.org/terms_use.jsp

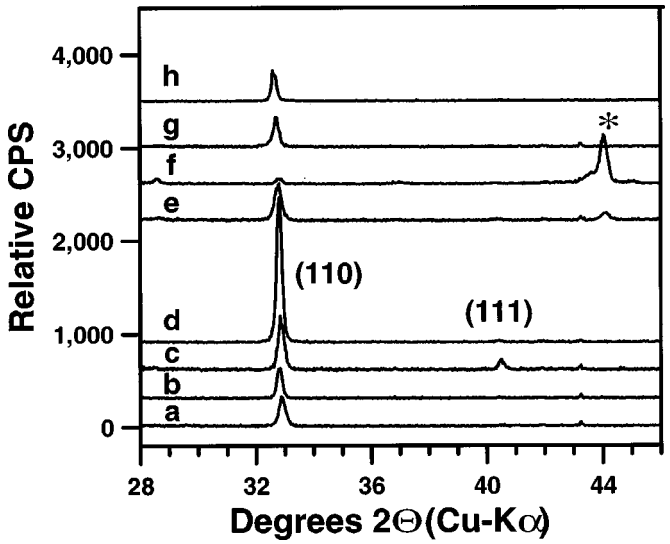

Figure 1. X-ray spectra for 300 nm thin films of $SrFe_{0.5}Co_{0.5}O_x$ on sapphire: (a) $SrFeO_x$; (b) $SrFe_{0.9}Co_{0.1}O_x$; (c) $SrFe_{0.75}Co_{0.25}O_x$; (d) $SrFe_{0.5}Co_{0.5}O_x$; (e) $SrFe_{0.25}Co_{0.75}O_x$; (f) $SrCoO_x$; (g) $SrFe_{1.0}Co_{0.5}O_x$; and (h) $SrFe_{1.3}Co_{0.2}O_x$. Indexing is given for the cubic perovskite structure; (*) indicates (201) $SrCoO_x$ hexagonal phase indexing.

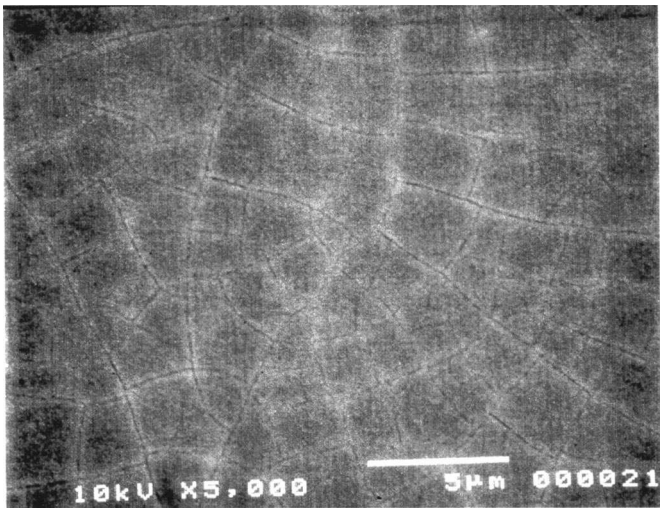

Figure 2. SEM micrograph of an as-deposited 300 nm $SrFe_{0.75}Co_{0.25}O_x$ film.

$SrFe_{1.3}Co_{0.2}O_x$ were both indexed to an orthorhombic phase, which is an intergrowth of repeating layers of perovskite and rock-salt layers.[9,12,30]

Two series of $SrFe_yCo_zO_x$ thin films on $(1\bar{1}02)$ single-crystal sapphire substrates were prepared by laser deposition using a Lambda-Physik LPX305i laser operating at $\lambda = 248$ nm. These included the solid solution perovskite series $SrFe_yCo_{1-y}O_x$ ($y = 0$, 0.25, 0.5, 0.75, 0.9, 1.0) and the structurally related materials $SrFe_{1.0}Co_{0.5}O_x$ and $SrFe_{1.3}Co_{0.2}O_x$. For each composition, the films were deposited at two separate thicknesses, approximately 30 and 300 nm. A laser pulse rate of 8 Hz was used with an energy density at the target of 1.5 J cm^{-2}. During the deposition step, the sapphire substrate was heated at 700°C under a background gas of 13 Pa oxygen, followed by cooling at approximately 10°C/min in a background oxygen pressure of 53 kPa.

X-ray spectra for both pellets and films were collected using a Cu Kα Scintag XDS2000 diffractometer with a secondary beam graphite monochromator over the range $20 \leqslant 2\theta \leqslant 80°$. The very intense peaks from the single-crystal sapphire substrate also showed satellite peaks arising from W-L_α and W-L_β X-rays originating from the W filament in the X-ray tube. The very weak peak at $2\theta = 43.24°$ (Fig. 1) is attributable to such a satellite peak. Film thicknesses were estimated based on stylus profiler measurements taken with a Dektak IIA instrument on masked 300 nm $SrFe_yCo_zO_x$ thin films grown on sapphire. Elemental analysis for targets and films were performed by inductively coupled plasma atomic emission spectroscopy (ICP-AES) using standard solutions to determine the ratio of Sr, Fe, and Co elements. Scanning electron microscopy (SEM) images were taken of the as-deposited films using a JEOL JSM 5300 instrument.

Electrical conductivity measurements of the films were taken using a two-wire method in a controlled environment where the temperature could be varied between 20 and 600°C and the composition of the flowing gas changed as required. High-purity ($[O_2] + [N_2] > 99.99\%$) gas mixtures flowing at 220 cm^3/min in a 1 L volume chamber were used for all tests. Electrical contacts were achieved by thermally depositing 200 nm Au pads directly onto the $SrFe_yCo_{1-y}O_x$ films. Sheet resistances and conductivities of the films were calculated from the resistance measurement and corrected for the geometrical configuration of the Au electrode pads and the thickness of the film.[31] Experimental details are provided elsewhere.[23,25]

In order to determine the dynamic temperature dependences, the resistances of the films were measured while cooling at a controlled rate of 10°C/min from 500 to 100°C. Prior to this, the films were equilibrated at 500°C for at least 3 h in one of two flowing O_2/N_2 gas mixtures: 0.2% O_2 or 100% O_2. The composition of the flowing gas mixture was invariant throughout the cooling cycle. For each film, this procedure was repeated at least twice to ensure reproducibility. The conductivities of the films as a function of the O_2/N_2 gas mixtures were measured isothermally at 500°C. This was done by measuring the film resistances as the O_2/N_2 gas mixtures were varied from oxygen-poor (~0.01% O_2) to oxygen-rich (100% O_2) conditions in a stepwise manner, typically waiting 60 min before changing to the next O_2/N_2 gas composition. The gas mixtures were then changed in the reverse order from oxygen-rich to oxygen-poor in order to verify reversibility.

Results and Discussion

Film composition and structure.—XRD analysis of the 300 nm films deposited on sapphire showed the films to be crystalline and textured (Fig. 1). No reflections for the 30 nm films were observed except for the very strong sapphire reflections from the substrate due to the small sample thickness of these films. The $SrFe_yCo_{1-y}O_x$ ($y = 0.5$, 0.75, 0.9, 1.0) films were all indexed to the cubic perovskite structure[26] and were (110) textured. The $SrFe_{0.75}Co_{0.25}O_x$ film showed an additional degree of (111) texturing. The $SrCoO_x$ film (Fig. 1f) was indexed to the $SrCoO_x$ hexagonal structure and was textured (201).[29] It was not clear from the $SrFe_{0.25}Co_{0.75}O_x$ film (Fig. 1e) whether it adopted the cubic perovskite or the hexagonal structure. Likewise, the $SrFe_{1.0}Co_{0.5}O_x$ and $SrFe_{1.3}Co_{0.2}O_x$ films could not be unambiguously assigned to the expected orthorhombic phase, since the reflection at $2\theta \approx 32.7°$ could be indexed to either the (110) reflection of the cubic perovskite structure or to the composite (400) + (002) or (251) reflections of the orthorhombic phase.[9,12,30]

SEM analysis of all the 30 nm films showed the films to be featureless and smooth at a length scale ≥0.1 μm. The 300 nm films showed grain boundaries and/or scales at a length scale (l) of $1 \leqslant l \leqslant 5$ μm for $SrFe_yCo_{1-y}O_x$ ($y = 0.25$, 0.5, 0.75, 0.9, 1.0) compositions. For example, micrographs of the 300 nm $SrFe_{0.75}Co_{0.25}O_x$ film clearly showed 1-3 μm cracks or scales (Fig. 2). The $SrCoO_x$, $SrFe_{1.0}Co_{0.5}O_x$, and $SrFe_{1.3}Co_{0.2}O_x$ films showed no evidence of scaling but showed some roughness at a length scale

Downloaded 03 Jun 2009 to 132.246.79.102. Redistribution subject to ECS license or copyright; see http://www.ecsdl.org/terms_use.jsp

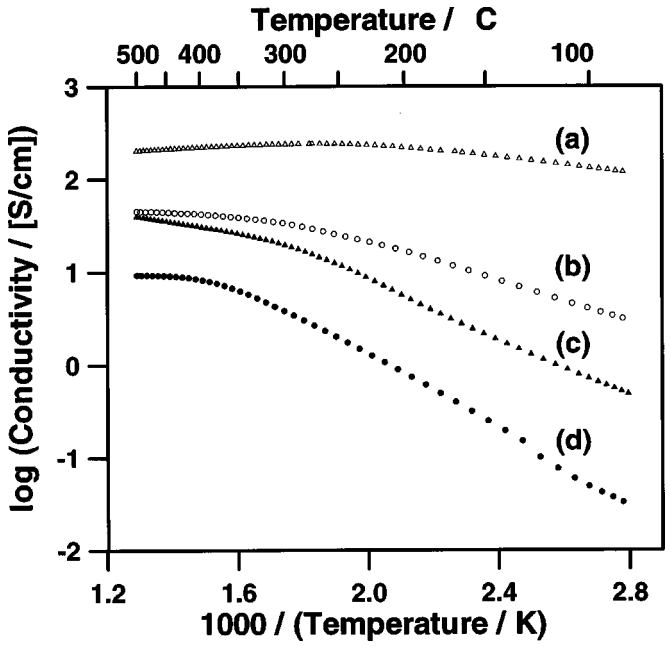

Figure 3. Arrhenius plots for two 30 nm films in different O_2/N_2 mixtures: $SrFe_{0.25}Co_{0.75}O_x$ in (a) 100% and (c) 0.2% O_2; and $SrFeO_x$ in (b) 100% and (d) 0.2% O_2.

of $0.1 \leqslant l \leqslant 0.3$ μm. Elemental analysis of the films showed that the Sr, Fe, and Co metallic elements occurred in the correct ratios to within the 5% estimated error limits of the ICP-AES technique. XRD, elemental, and SEM analyses confirmed that PLD is a suitable technique for the stoichiometric transfer of material from the target to the substrate for heterometallic oxides such as mixed conducting $SrFe_yCo_zO_x$ ceramics.

Dependence of temperature on film conductivity.—The conductance response to temperature for two 30 nm thick films ($SrFeO_x$ and $SrFe_{0.25}Co_{0.75}$) is shown in Fig. 3 as a set of Arrhenius plots. The higher conductivity of both films in 100% O_2 compared to 0.2% O_2 confirms that these materials are p-type semiconducting oxides.[18] It is also evident that the conductance response to temperature is much smaller for $SrFe_{0.25}Co_{0.75}$ than for $SrFeO_x$, especially in the temperature range $200 \leqslant T \leqslant 500$°C. An activation energy parameter, E_A, related to this temperature dependence of film conductance has been extracted from the Arrhenius plots of the entire $SrFe_yCo_{1-y}O_x$ series of films. The results summarized in Table I show the E_A values which were calculated for two temperature ranges. The $350 \leqslant T \leqslant 500$°C "nonstoichiometric" range was chosen since at these temperatures, bulk oxygen equilibration of the film is possible. Consequently, the balancing of the thermal activation of charge carriers effect with the "nonstoichiometric" effect can occur (Eq. 1-2). By comparison, the $100 \leqslant T \leqslant 200$°C "stoichiometric" range was chosen since the oxygen stoichiometry for the films is expected to be quenched when the experimental cooling rate of 10°C/min was used.

In general, a higher level of cobalt substitution results in smaller temperature dependences, with the smallest E_A values reported for the $SrFe_{0.75}Co_{0.25}O_x$, $SrFe_{0.5}Co_{0.5}O_x$, and $SrFe_{0.25}Co_{0.75}O_x$ films. It is also noteworthy that the temperature dependences of the films exposed to 0.2% O_2 are generally greater than those exposed to 100% O_2. This effect of decreased temperature dependence with oxygen content is consistent with other p-type perovskite materials including $SrFeO_x$[25,32] and $(Ba,Sr)Fe_{1-x}Ta_xO_3$.[18-21]

A significant influence of film thickness on the temperature dependence is also evident from Table I. In the nonstoichiometric region, $350 \leqslant T \leqslant 500$°C, reduced temperature dependence for the thinner films is indicated by smaller E_A values. Some of these values are even negative, indicating that a decreased temperature actually results in an increased conductance. This phenomenon has previously been reported for other mixed oxide perovskites, albeit at higher temperatures.[18-21] Figure 4 illustrates how the film thickness can influence the temperature-dependent conduction response. The thinner 30 nm film has a smaller temperature dependence over a larger temperature range. This may be the result of a higher surface area-to-volume ratio for the thinner film, resulting in faster bulk oxygen equilibration, or to an effect related to the degree of interfacial stress between the substrate and the film.

All the E_A values were extracted from the slopes of Arrhenius plots (Eq. 1) for cooling ramps of 10°C/min under an invariant composition of the O_2/N_2 gas mixture. At some point during cool-

Table I. Activation energies of conduction, E_A, for $SrFe_yCo_zO_x$ films on sapphire in the "nonstoichiometric" (350-500°C) and "stoichiometric" (200-100°C) temperature ranges. E_A values were derived from dynamic 10°C/min temperature cooling ramps.

Composition	Thickness (nm)	E_A, eV (350-500°C) 100% O_2	E_A, eV (350-500°C) 0.2% O_2	E_A, eV (100-200°C) 100% O_2	E_A, eV (100-200°C) 0.2% O_2
$SrFeO_x$	300	0.39	0.39	0.23	0.47
	30	0.04	0.09	0.22	0.44
$SrFe_{0.9}Co_{0.1}O_x$	300	0.37	0.19	0.28	0.49
	30	0.10	0.12	0.22	0.39
$SrFe_{0.75}Co_{0.25}O_x$	300	0.20	−0.04	0.18	0.31
	30	−0.02	0.01	0.13	0.29
$SrFe_{0.5}Co_{0.5}O_x$	300	0.13	0.10	0.12	0.26
	30	−0.04	−0.003	0.12	0.26
$SrFe_{0.25}Co_{0.75}O_x$	300	0.002	0.04	0.16	0.25
	30	−0.04	0.12	0.08	0.31
$SrCoO_x$	300	0.06	0.02	0.15	0.18
	30	0.07	−0.005	0.17	0.17
$SrFe_{1.3}Co_{0.2}O_x$	300	0.08	0.21	0.22	0.34
	30	0.23	0.31	0.25	0.39
$SrFe_{1.0}Co_{0.5}O_x$	300	0.02	0.10	0.19	0.32
	30	0.07	0.064	0.19	0.29

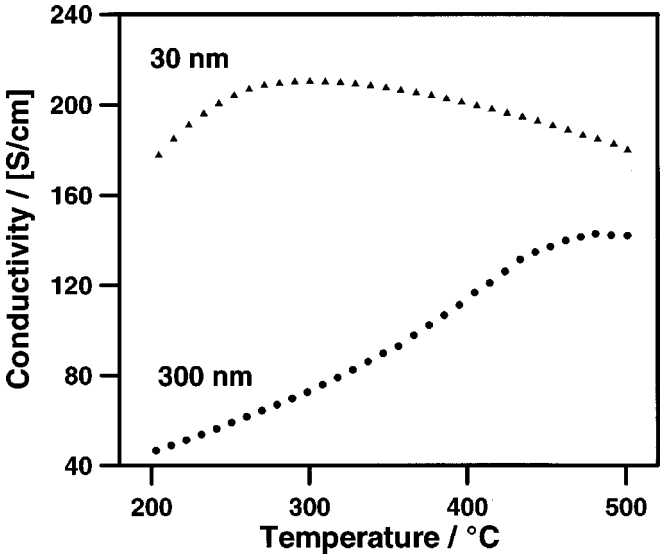

Figure 4. Effects of film thickness on the conductance response with temperature for two $SrFe_{0.5}Co_{0.5}O_x$ films: (▲) 30 and (●) 300 nm. Cooling ramps were carried out in 100% O_2 at 10°C/min.

Downloaded 03 Jun 2009 to 132.246.79.102. Redistribution subject to ECS license or copyright; see http://www.ecsdl.org/terms_use.jsp

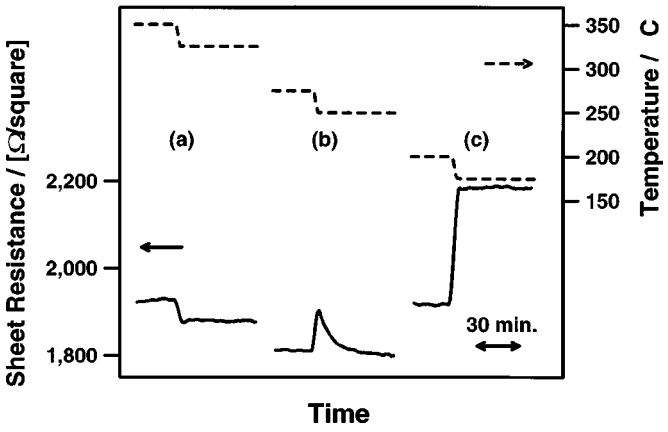

Figure 5. Dynamic temperature response of resistance for 30 nm films of $SrFe_{0.25}Co_{0.75}O_x$ in 20% O_2 for (a) 350-325°C, (b) 275-250°C, and (c) 200-175°C. Cooling ramps were conducted at 10°C/min.

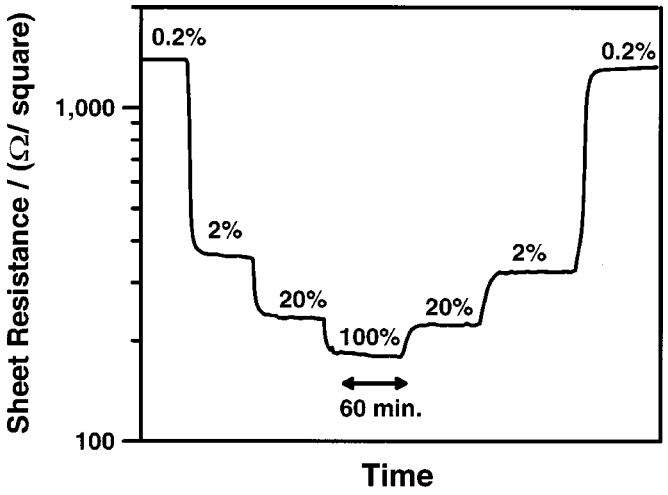

Figure 6. Resistance response to variations in O_2/N_2 gas composition (% O_2) for a 300 nm $SrFe_{0.5}Co_{0.5}O_x$ film at 500°C.

ing, chemical equilibrium between the film and the surrounding gas mixture cannot be maintained as the kinetics of O_2 exchange slows down and quenching occurs. The temperature at which quenching occurs is dependent on both film composition, thickness, and cooling rate. Figure 5 shows the resistance response when a $SrFe_{0.25}Co_{0.75}O_x$ film is first equilibrated in air at three different temperatures between 200 and 350°C in air, cooled by 25°C at 10°C/min, followed by re-equilibration at the new temperature. At higher temperatures (Fig. 5a) the system maintains equilibrium throughout the 10°C/min cooling rate. Cooling results in an immediate decrease in film resistance resulting from the dominant role of the nonstoichiometric effect (Eq. 2). When the temperature is at an intermediate range (Fig. 5b), the resistance of the film initially increases with decreasing temperature, as would be expected on the basis of thermally activated charge carriers. Once the final temperature is reached, the resistance no longer continues to increase but instead decreases. This is due to the nonstoichiometric effect, where the film continues to react with the oxygen from the surrounding gas mixture, resulting in an increased number of hole charge carriers. At this intermediate temperature range, bulk equilibration still occurs, although too slow for equilibrium to be maintained during the cooling step. At lower temperatures (Fig. 5c), quenching occurs and the oxygen stoichiometry of the film does not change. As a result, the balancing of thermal effects cannot occur, and the material behaves as a normal semiconductor, where decreasing temperature results in increased resistance.

Oxygen-sensing properties of $SrFe_yCo_zO_x$ thin films.—The effects on conductivity of varying the O_2/N_2 composition at $T = 500$°C was examined for all of the $SrFe_yCo_zO_x$ films. Figure 6 shows a typical example where the composition of the O_2/N_2 gas mixture was changed stepwise from 0.2% O_2 to 100% O_2 and back to 0.2% O_2. At 500°C, the resistance response to variations in oxygen composition is rapid and reversible. The response is faster when the O_2 concentration is increasing compared to when the O_2 concentration is decreasing. The response time is determined in part by the relatively slow mixing time for the 220 cm^3/min gas mixtures in the 1 L volume of the chamber. The results of the isothermal variation of O_2/N_2 gas mixtures for the $SrFe_yCo_{1-y}O_x$ set of films are summarized in Fig. 7-10. The results for the $SrFe_{1.0}Co_{0.5}O_x$ and $SrFe_{1.3}Co_{0.2}O_x$ films are summarized in Fig. 11.

In all cases, exposure to increasing oxygen concentration levels resulted in increased film conductivity, as would be expected for p-type semiconducting oxides. Film conductivities at 500°C ranged between 20 and 200 S/cm for films exposed to 100% O_2 atmosphere and 0.4-25 S/cm for films exposed to 0.01% O_2. The conductivity of the films increased with increasing cobalt substitution of the $SrFeO_x$ parent material up to a maximum value. This maximum occurred within the range of composition $SrFe_yCo_{1-y}O_x$ ($0.25 \leqslant y \leqslant 0.75$) and was dependent on film thickness and the composition of the gas mixture. The $SrFe_{1.0}Co_{0.5}O_x$ and $SrFe_{1.3}Co_{0.2}O_x$ set of films also showed that cobalt substitution resulted in increased conductivity. There were some subtle differences between the 30 nm series (Fig. 7 and 9) and the 300 nm (Fig. 8 and 10) series of films, including differences in the composition where maximum conductivities were observed. This is possibly an effect of the increased role of interfacial stress between the film and the substrate, or is due to the increasing contribution of the space-charge regions at the interfaces for the thinner films.

The sensitivity of the film to oxygen with respect to its change in conductivity may be represented as the slope of the log{conductivity} *vs.* log{p_{O_2}} plot. This slope corresponds to a parameter $1/N$, where N is a constant determined by the dominant type of bulk defect involved in the equilibrium between oxygen and the

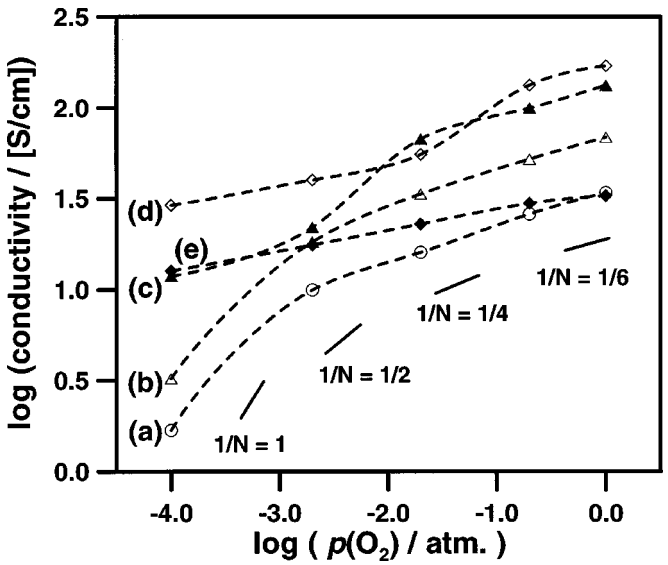

Figure 7. Conductivity of a $SrFe_yCo_{1-y}O_x$ series of 30 nm films at 500°C for different O_2/N_2 gas compositions. 1/N represents different slopes of the log(σ) *vs.* log p_{O_2} relationship. (a, -○-) $SrFeO_x$; (b, -△-) $SrFe_{0.75}Co_{0.25}O_x$; (c, -▲-) $SrFe_{0.5}Co_{0.5}O_x$; (d, -◇-) $SrFe_{0.25}Co_{0.75}O_x$; and (e, -◆-) $SrCoO_x$.

Downloaded 03 Jun 2009 to 132.246.79.102. Redistribution subject to ECS license or copyright; see http://www.ecsdl.org/terms_use.jsp

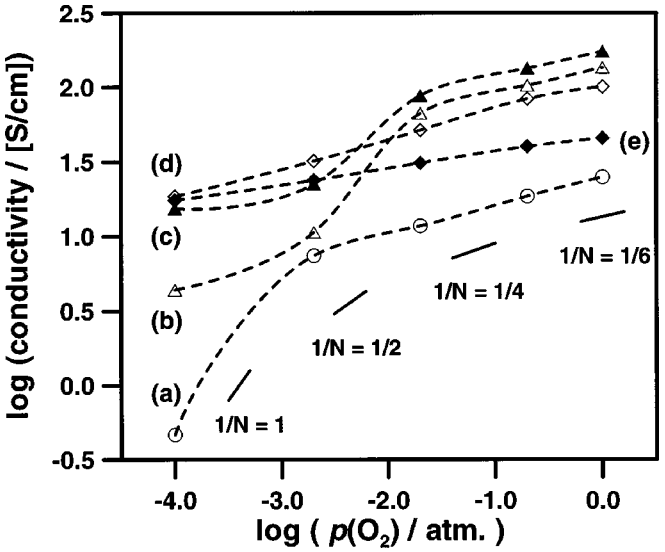

Figure 8. Conductivity of a $SrFe_yCo_{1-y}O_x$ series of 300 nm films at 500°C for different O_2/N_2 gas compositions. 1/N represents different slopes of the log(σ) *vs.* log p_{O_2} relationship. (a, -○-) $SrFeO_x$; (b, -△-) $SrFe_{0.75}Co_{0.25}O_x$; (c, -▲-) $SrFe_{0.5}Co_{0.5}O_x$; (d, -◇-) $SrFe_{0.25}Co_{0.75}O_x$; and (e, -◆-) $SrCoO_x$.

sensor.[18] The oxygen sensitivity of the films ranged from $0.05 \leqslant 1/N \leqslant 0.9$ (Fig. 7, 8, and 11). For some films, including $SrFe_{0.5}Co_{0.5}O_x$ and $SrFe_{0.75}Co_{0.25}O_x$, enhanced oxygen sensitivity was observed over narrow p_{O_2} regions, as indicated by the increased slope between two consecutive points in the log{conductivity} *vs.* log{p_{O_2}} plots. Alternately, this was also evident from anomalous large spacings between consecutive isobars shown in Fig. 9 and 10.

Enhanced oxygen sensitivity of $SrFeO_{2.5+x}$ has been previously attributed to phase transitions between the brownmillerite and cubic perovskite phases.[25] At 500°C this phase transition is expected to occur at $0.005 \leqslant (O_2) \leqslant 0.05$ atm.[25-27] Liu *et al.*[33] have also identified a similar phase transition for $SrFe_{0.2}Co_{0.8}O_x$ below 750°C for $0.05 \leqslant p_{O_2} \leqslant 0.20$ atm. The sensitivity of the films to oxygen between $0.002 \leqslant p_{O_2} \leqslant 0.02$ atm for the series of $SrFe_yCo_{1-y}O_x$ films is shown in Fig. 12. For the 300 nm films, high oxygen sensitivity is observed for both the $SrFe_{0.5}Co_{0.5}O_x$ and

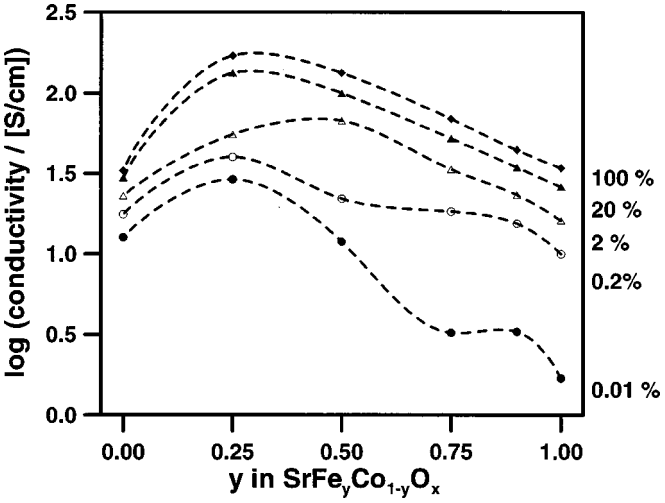

Figure 9. The effects of cobalt substitution and O_2/N_2 gas composition (% O_2) on conductivity for a series of 30 nm $SrFe_yCo_{1-y}O_x$ films at 500°C.

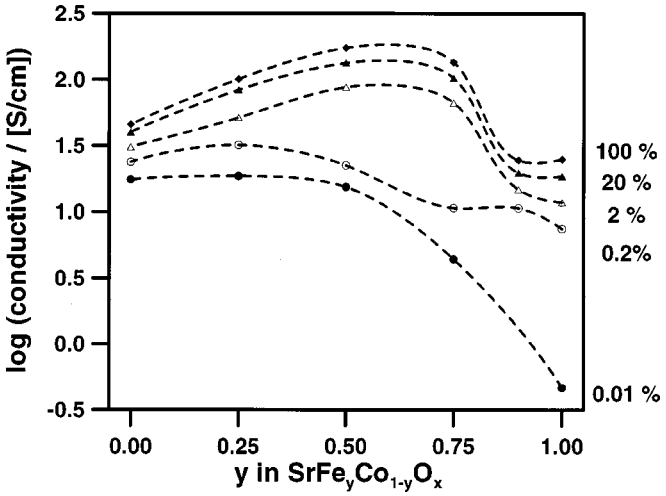

Figure 10. The effects of cobalt substitution and O_2/N_2 gas composition (% O_2) on conductivity for a series of 300 nm thick $SrFe_yCo_{1-y}O_x$ films at 500°C.

$SrFe_{0.75}Co_{0.25}O_x$, whereas it is only observed for $SrFe_{0.5}Co_{0.5}O_x$ for the 30 nm films. This demonstrates that film thickness influences to some extent, the sensitivity of the film to oxygen.

Sensing reducing gases with $SrFe_yCo_zO_x$ thin films.—It has previously been shown that $SrFeO_x$ films may used to detect reducing gases in air by monitoring the change in film resistance with gas exposure.[34] This is also the case for $SrFe_yCo_zO_x$ thin films. Figure 13 shows the resistance response of a 30 nm $SrFe_{0.25}Co_{0.75}Ox$ film to exposure to H_2, CO, and CH_4 in background air at 300°C. The film shows good sensitivity to H_2, moderate sensitivity to CO, and negligible sensitivity to CH_4. The operating temperature of 300°C was selected for this film because in a background atmosphere of air, this film exhibits very little temperature dependence for its resistance response. The speed of response is relatively slow at 300°C. The time required for 90% of the change of resistance to occur (t_{90})

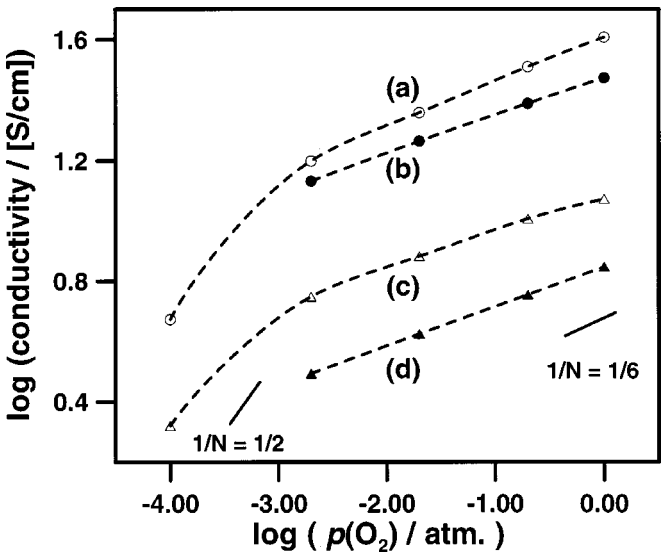

Figure 11. Conductivity of $SrFe_{1.5-z}Co_zO_x$ films at 500°C for different O_2/N_2 gas compositions and different thicknesses. 1/N represent different slopes of the log(σ) *vs.* log p_{O_2} relationship: (a) $SrFe_{1.0}Co_{0.5}O_x$ 30 nm; (b) $SrFe_{1.0}Co_{0.5}O_x$ 300 nm; (c) $SrFe_{1.3}Co_{0.2}O_x$ 30 nm; and (d) $SrFe_{1.3}Co_{0.2}O_x$ 300 nm.

Downloaded 03 Jun 2009 to 132.246.79.102. Redistribution subject to ECS license or copyright; see http://www.ecsdl.org/terms_use.jsp

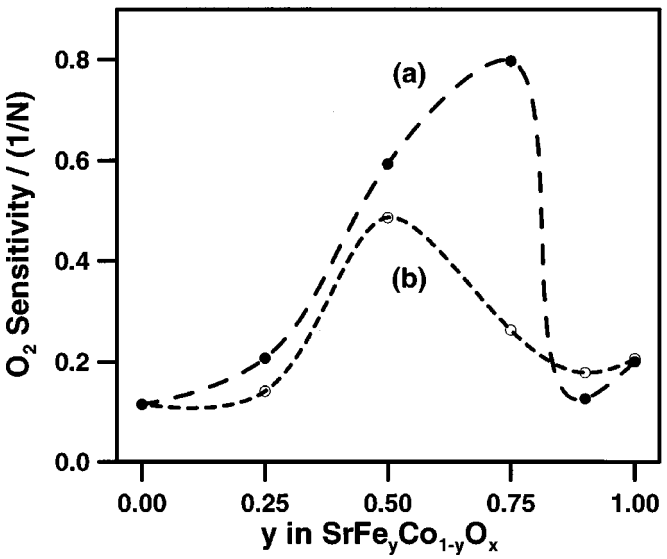

Figure 12. Effects of cobalt substitution on oxygen sensitivity at 500°C for the $SrFe_yCo_{1-y}O_x$ series of films at two thicknesses: (a) 30 and (b) 300 nm. Sensitivities were calculated between 0.2 and 2% O_2.

is typically between 10 and 15 min. The slow response time is a consequence of its dependence on the bulk equilibration of the film with oxygen and not only surface interactions. Nonetheless, it is possible to use this film to detect reducing gases in air at a temperature not normally associated with gas sensors based on bulk equilibration, which normally operates above 500°C.[18] Moreover, at this temperature, the film is operating in nearly a temperature-independent region.

Conclusions

It has been demonstrated that thin films of $SrFe_yCo_zO_x$ grown by PLD exhibit novel conductivity responses with respect to variation in both temperature and gas composition. Due to the balancing of thermal effects, it is possible to obtain a conduction response which has a negligible temperature dependence between $200 \leqslant T \leqslant 500$°C. This effect was most pronounced for the perovskites with compositions $SrFe_{0.25}Co_{0.75}O_x$ and $SrFe_{0.5}Co_{0.5}O_x$. Thinner films (30 nm) show a greater temperature independence than the thicker (300 nm) films at temperature between $350 \leqslant T \leqslant 500$ °C. All the $SrFe_yCo_zO_x$ films showed reversible p-type gas sensor responses at 500°C to variations in O_2/N_2 gas mixtures. Regions of enhanced oxygen sensitivity over narrow p_{O_2} ranges were attributed to phase transitions between the cubic perovskite and brownmillerite phases. Finally, it was shown that it is possible to use $SrFe_yCo_zO_x$ films to detect H_2 and CO in background air while operating under conditions where there is negligible temperature dependence.

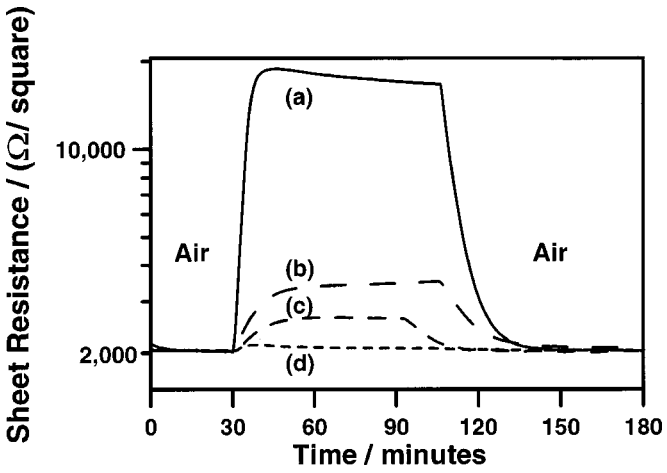

Figure 13. Resistance response at 300°C of a 30 nm $SrFe_{0.50}Co_{0.50}O_x$ film to (a) 1% CO; (b) 1000 ppm CO; (c) 1% H_2; and (d) 1000 ppm CH_4 in background air.

Acknowledgments

The authors are grateful to G. Pleizier for the SEM analysis of the thin films, and V. Boyko for the elemental analysis measurements by ICP-AES.

The National Research Council of Canada assisted in meeting the publication costs of this article.

References

1. Y. Teraoka, H.-M. Zhang, S. Furukawa, and N. Yamazoe, *Chem. Lett.,* **1985**, 1743.
2. Y. Teraoka, T. Nobunaga, and N. Yamazoe, *Chem. Lett.,* **1988**, 503.
3. Y. Teraoka, H. M. Zhang, K. Okamoto, and N. Yamazoe, *Mater. Res. Bull.,* **23**, 51 (1988).
4. V. V. Kharton, E. N. Naumovitch, and A. V. Nikolaev, *J. Membr. Sci.,* **111**, 149 (1996).
5. V. V. Kharton, V. N. Tikhonovitch, L. Shuangbao, E. N. Naumovitch, A. V. Kovalevsky, A. P. Viskup, I. Bashmakov, and A. A. Yaremchenko, *J. Electrochem. Soc.,* **145**, 1363 (1998).
6. L. V. Kokhanovskii, V. V. Vashuk, E. F. Vil'kotshaya, S. I. Vitushko, and M. V. Zinkevich, *Inorg. Mater. (Transl. of Neorg. Mater.),* **35**, 282 (1999).
7. L. Qiu, T. H. Lee, L. M. Jiu, Y. L. Yang, and A. J. Jacobson, *Solid State Ionics,* **76**, 321 (1995).
8. T. Armstrong, F. Prado, Y. Xia, and A. Manthiram, *J. Electrochem. Soc.,* **147**, 435 (2000).
9. S. Guggilla and A. Manthiram, *J. Electrochem. Soc.,* **144**, L120 (1997).
10. J. W. Stephenson, T. R. Armstrong, R. D. Carneim, L. R. Pederson, and W. J. Weber, *J. Electrochem. Soc.,* **143**, 2722 (1996).
11. U. Balachandran, B. Ma, P. S. Maiya, R. L. Mieville, J. T. Dusek, J. J. Picciolo, J. Guan, S. E. Dorris, and M. Liu, *Solid State Ionics,* **108**, 363 (1998).
12. B. Ma, U. Balachandran, J. H. Park, and C. U. Segre, *Solid State Ionics,* **83**, 65 (1996).
13. B. Ma, U. Balachandran, J. H. Park, and C. U. Segre, *J. Electrochem. Soc.,* **143**, 1736 (1996).
14. B. Ma and U. Balachandran, *Solid State Ionics,* **100**, 53 (1997).
15. B. Ma and U. Balachandran, *J. Electroceram.,* **2**, 135 (1998).
16. B. J. Mitchell, J. W. Richardson, C. D. Murphy, B. Ma, U. Balachandran, J. P. Hodges, and J. D. Jorgensen, *Mater. Res. Bull.,* **35**, 491 (2000).
17. B. Ma and U. Balachandran, *Mater. Res. Bull.,* **33**, 223 (1998).
18. P. T. Moseley and A. J. Crocker, *Sensor Materials*, Chap. 4, Institute of Physics Publishing, Ltd., London (1996).
19. P. T. Moseley and D. E. Williams, *Polyhedron,* **8**, 1615 (1989).
20. D. E. Williams, B. C. Tofield, and P. McGeehin, Euro. Pat. EP62-994 and U.S. Pat. 4,454,494 (1982).
21. R. Moos, W. Menesklou, H.-J. Schreiner, and K. H. Härdtl, *Sens. Actuators B,* **67**, 178 (2000).
22. M. L. Post, B. W. Sanders, and P. Kennepohl, *Sens. Actuators B,* **13-14**, 272 (1993).
23. M. L. Post, J. J. Tunney, and J. Yao, in *Chemical and Biological Sensors and Analytical Electrochemical Methods*, A. J. Ricco, M. A. Butler, P. Vanysek, G. Horvai, and A. F. Silva, Editors, PV 97-19, p. 889, The Electrochemical Society Proceedings Series, Pennington, NJ (1997).
24. M. L. Post, J. J. Tunney, D. Yang, X. Du, and D. L. Singleton, *Sens. Actuators B,* **59**, 90 (1999).
25. J. J. Tunney and M. L. Post, *J. Electroceram.,* **5**, 63 (2000).
26. Y. Takeda, K. Kanno, T. Takada, O. Yamamoto, M. Takano, N. Nakayama, and Y. Bando, *J. Solid State Chem.,* **63**, 237 (1986).
27. J. Mizusaki, M. Okayasu, S. Yamauchi, and K. Fueki, *J. Solid State Chem.,* **99**, 166 (1992).
28. J. P. Hodges, S. Short, J. D. Jorgensen, X. Xiong, B. Dabrowski, S. M. Mini, and C. W. Kimball, *J. Solid State Chem.,* **151**, 190 (2000).
29. Y. Takeda, R. Kanno, T. Takada, O. Yamamoto, M. Takano, and Y. Bando, *Z. Anorg. Allg. Chem.,* **540/541**, 259 (1986).
30. H. Fjellvag, B. C. Hauback, and R. Bredesen, *J. Mater. Chem.,* **1997**, 2415.
31. L. I. Maissel, in *Handbook of Thin Film Technology*, L. I. Maissel and R. Glang, Editors, Chap. 13, McGraw-Hill Book Co., New York (1970).
32. J. Hombo, Y. Matsumoto, and T. Kawano, *J. Solid State Chem.,* **84**, 138 (1990).
33. L. M. Liu, T. H. Lee, L. Qiu, Y. Yang, and A. J. Jacobson, *Mater. Res. Bull.,* **31**, 29 (1996).
34. M. L. Post, J. J. Tunney, D. Yang, and X. Du, in *Chemical Sensors IV*, M. Butler, N. Yamazoe, P. Vanysek, and M. Aizawa, Editors, PV 99-23, p. 270, The Electrochemical Society Proceedings Series, Pennington, NJ (1999).

Downloaded 03 Jun 2009 to 132.246.79.102. Redistribution subject to ECS license or copyright; see http://www.ecsdl.org/terms_use.jsp